Table I. Energetics of Electron-Transfer Pathways in Some Covalently Linked Transition Metal Complexes[a]

| complex | $k_{BET}$(obsd), $s^{-1}/10^{10}$ | $\Delta G^{\circ}$ [b] | $\lambda$[c] | $\Delta G^{\ddagger}_{BET}$[d] | $k_{BET}$(calcd),[e] $s^{-1}/10^{12}$ |
|---|---|---|---|---|---|
| $(bpy)_2Ru((CN)Co(NH_3)_5)_2^{6+}$ | 0.3 | 12.3[f] | 15 ± 3[f] | 0.0-0.3<br>0.11 | 2-11 |
| $(bpy)_2(CN)Ru((CN)Co(tetraen))^{3+}$ | 0.4 | 11.8 | 14 ± 2 | 0.0-0.03<br>0.09 | 2-11 |
| $(bpy)_2(CN)Ru((CN)Co(terpy)(bpy))^{3+}$ | 0.3 | 8.0 | 11 ± 2 | 0.00-0.2 | 5-12 |
| $(bpy)_2Ru((CN)Ru(NH_3)_5)_2^{6+}$ [g] | >2 | 11.3 | 3 | (4)[h] | $(2 \times 10^{-7})$ |
| $(NC)_5Fe((CN)Ru(NH_3)_5)^{-}$ | >300[i] | 4.8[j] | 5.4 | 0.02 | 1 |

[a] Energies in $cm^{-1}/10^3$); temperature 25 °C in acetonitrile except as indicated. [b] Based on cyclic voltametric measurements except as indicated. [c] Nuclear reorganizational parameter; $\lambda = \lambda_s + \lambda_v$, where $\lambda_s$ originates from solvational changes and $\lambda_v$ from metal-ligand bonding changes (refs 7). Calculated values from ref 8g and work in progress. The error limits are based on the propagation of error in the calculated values. [d] Based on $\Delta G^{\ddagger} = (\lambda/4)(1 + \Delta G^{\circ}/\lambda)^2$; refs 7. Range of values based on the error limits for $\lambda$. [e] $k_{BET}$(calcd) = $\kappa_{nu}\nu_{eff}$, $\kappa_{nu} = \exp(-\Delta G^{\ddagger}_{BET}/RT)$; see refs 7. Range of values based on the range of $\Delta G^{\ddagger}$ values. [f] Estimate based on $Co(NH_3)_6^{3+,2+}$ parameters: refs 8a,d,g. [g] Prepared and characterized as described by Bignozzi et al.: Bignozzi, C. A.; Roffia, S.; Scandola, F. *J. Am. Chem. Soc.* **1985**, *107*, 1644. [h] The classical model often predicts too large an activation barrier for the "Marcus inverted region" ($|\Delta G^{\circ}| > \lambda$); refs 7. [i] Ref 4. [j] Ref 3.

here is among the strongest evidence to date that electronic factors can inhibit thermally activated electron transfer.

We used three cyanometalates of $Ru(bpy)_2(CN)_2$ in these studies: (a) $(bpy)_2Ru((CN)Co(NH_3)_5)_2^{6+}$; (b) $(bpy)_2(CN)Ru((CN)Co(tetraen))^{3+}$; and (c) $(bpy)_2(CN)Ru((CN)Co(terpy)(bpy))^{3+}$. Irradiations at the ruthenium(II) metal-to-ligand charge-transfer (MLCT) bands of these complexes in solution showed no evidence of the usual ruthenium emission.[9,10] The transient species, generated by an 18-ps, 532-nm excitation of the complex in water or acetonitrile, absorbed much less in the 400-500-nm (Ru(II) → bpy MLCT) region and more strongly at longer wavelengths than did the substrates. These transients decayed smoothly to regenerate the substrate absorbancies in about 1 ns.[11] The observed absorbance changes demonstrate photoinduced charge separation followed by simple BET to form the original Ru(II)-Co(III) ground states.[12]

The BET processes in these Ru-Co systems have very small activation barriers ($\Delta G^{\ddagger}$ (calcd) ≤300 $cm^{-1}$; see Table I). Simple electron-transfer models suggest that the BET process should be about 1000 times faster than observed (Table I). Simple cyano-bridged, Fe-Ru and Ru-Ru (Table I) systems, in which no electronic retardation is expected, exhibit much faster BET rates.[3,4] Thus, the relatively small observed values of $k_{BET}$ for the Ru-Co systems implicates an electronic retardation factor of $\kappa_{el} \sim 10^{-3}$-$10^{-4}$ for the $(^2T_2)Ru(III)-(^4T_2)Co(II) \rightarrow (^1A_1)Ru(II)-(^1A_1)Co(III)$ electron-transfer process.

The apparent acceptor independence of $k_{BET}$ was unexpected. While the large driving forces of the BET process should lead to very small values of the classical activation energy and little variation in the nuclear retardation factor $\kappa_{nu} = \exp(-\Delta G^{\ddagger}/RT)$, the $(^4T_2)Co(II) - (^2E)Co(II)$ energy difference should vary in these complexes,[13,14] leading to significant variations in $\kappa_{el}$.[15] That this is not the case may be due to a cancellation of contributions. It is also possible that the sensitivity of $\kappa_{el}$ in these rigid systems to donor-acceptor orbital symmetry ($\sigma$-donor and $\pi$-acceptor orbitals are involved here) modulates variations expected from spin-orbit coupling.

**Acknowledgment.** Partial support of this research from the Division of Chemical Sciences, Office of Basic Energy Research, U.S. Department of Energy, is gratefully acknowledged. We are very grateful to the Notre Dame Radiation Laboratory and Dr. Richard Fessenden for providing us with access to the picosecond flash photolysis system, and to Dr. John Chateauneuf for assisting us with this instrument.

**Supplementary Material Available:** Figure 1 depicting transient spectra of some RuCNCo complexes (1 page). Ordering information is given on any current masthead page.

(8) Recent discussions of various aspects of these issues can be found in the following: (a) Hammershoi, A.; Geselowitz, D.; Taube, H. *Inorg. Chem.* **1984**, *23*, 979. (b) Larsen, S.; Stähl, K.; Zerner, M. C. *Inorg. Chem.* **1986**, *25*, 3033. (c) Newton, M. D. In *The Challenge of d and f Electrons*; Salahub, D. R., Zerner, M. C., Eds.; ACS Symposium Series 394; American Chemical Society: Washington, DC, 1989; p 378. (d) Newton, M. D. *J. Phys. Chem.* **1991**, *95*, 30. (e) Ramasami, T.; Endicott, J. F. *J. Am. Chem. Soc.* **1985**, *107*, 389. (f) Endicott, J. F. *Acc. Chem. Res.* **1988**, *21*, 59. (g) Endicott, J. F.; Brubaker, G. R.; Ramasami, T.; Kumar, K.; Dwarakanath, K.; Cassel, J.; Johnson, D. *Inorg. Chem.* **1983**, *22*, 3754.

(9) (a) Lei, Y.; Buranda, T.; Endicott, J. F. *J. Am. Chem. Soc.* **1990**, *112*, 8821. (b) Lei, Y. Ph.D. Dissertation, Wayne State University, 1989.

(10) We observed greater than 95% emission quenching at both 298 and 77 K.

(11) A figure depicting characteristic transient spectra is in the supplementary material (see paragraph at end of paper). More complex behavior was observed for $(bpy)_2Ru((CN)Co(NH_3)_5)_2^{6+}$ in DMSO.

(12) The $(^3CT)Ru(bpy)^{2+}$ excited states of these dicyano species all exhibit strong absorbancies in the 430-460-nm region.[9] This absorption does not exist in Ru(III) complexes.

(13) The $^2E$ state has been estimated to be $13.7 \times 10^3$ $cm^{-1}$ above the ground $^4T_2$ state in $Co(NH_3)_6^{2+}$,[14] this energy difference is about $3.5 \times 10^3$ $cm^{-1}$ in $Co(bpy)_3^{2+}$.

(14) Lever, A. B. P. *Inorganic Electronic Spectroscopy*, 2nd ed.; Elsevier: New York, 1984.

(15) Newton, M. D. *Chem. Rev.* **1991**, *91*, 767.

## One-Electron Activation and Coupling of Ethene by Rhodium(II) Porphyrins: Observation of an $\eta^2$-Ethene-Metalloradical Complex

Andrew G. Bunn and Bradford B. Wayland*

*Department of Chemistry, University of Pennsylvania Philadelphia, Pennsylvania 19104-6323*

*Received April 6, 1992*

A series of rhodium(II) porphyrin ($d^7$, $s = {}^1/_2$) complexes where the ligand steric demands are incrementally increased has been used in studying metalloradical reactions of ethene. (Tetramesitylporphyrinato)rhodium(II),[1] (TMP)Rh•, and complexes with smaller ligand steric requirements react with ethene to form two-carbon alkyl bridged complexes, (por)Rh-$CH_2CH_2$-Rh(por).[2-5] Replacing the methyl substituents of TMP with ethyl and isopropyl groups results in rhodium(II) complexes that produce ethene coupling and permit observation of an intermediate $\eta^2$-ethene-metalloradical complex, [(por)Rh($CH_2$=$CH_2$)]•.

[Tetrakis(1,3,5-triethylphenyl)porphyrinato]rhodium(II), (TTEPP)Rh•, in benzene solution when exposed to ethene ($P_{C_2H_4} \sim 0.25$ atm) produces a four-carbon alkyl bridged complex, (TTEPP)Rh-$CH_2CH_2CH_2CH_2$-Rh(TTEPP) (**1**) (eq 1). Compound **1** is formed quantitatively within the time required to record

$$2(TTEPP)Rh^{\bullet} + 2CH_2{=}CH_2 \rightleftharpoons (TTEPP)Rh{-}CH_2CH_2CH_2CH_2{-}Rh(TTEPP) \quad (1)$$

(1) Wayland, B. B.; Sherry, A. E.; Poszmik, G.; Bunn, A. G. *J. Am. Chem Soc.* **1992**, *114*, 1673.

(2) Ogoshi, H.; Setsume, J.; Yoshida, Z. *J. Am. Chem. Soc.* **1977**, *99*, 3869.

(3) (a) Wayland, B. B.; Feng, Y.; Ba, S. *Organometallics* **1989**, *8*, 1438. (b) Sherry, A. E. Ph.D. Dissertation, University of Pennsylvania, 1990.

(4) Del Rossi, K. J.; Wayland, B. B. *J. Chem. Soc., Chem. Commun.* 1986, 1653.

(5) Paonessa, R. S.; Thomas, N. C.; Halpern, J. *J. Am. Chem. Soc.* **1985**, *107*, 4333.

0002-7863/92/1514-6917$03.00/0 

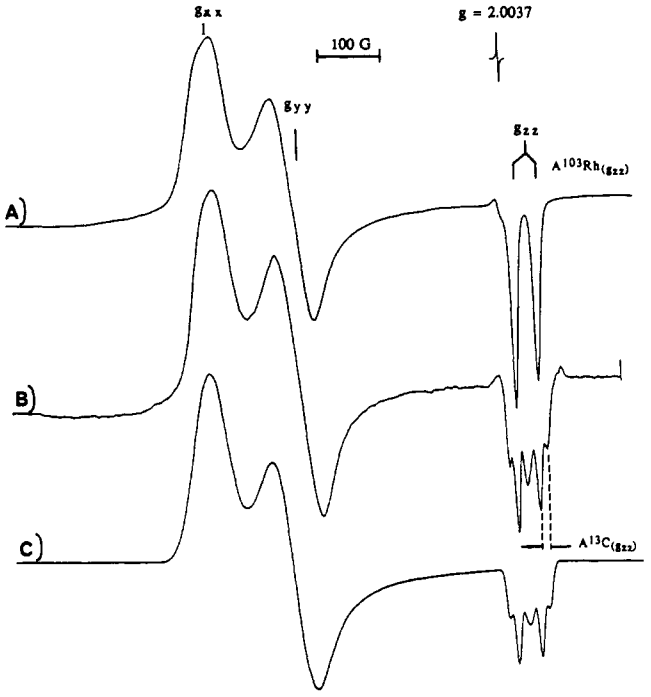


**Figure 1.** EPR spectra for $[(TTiPP)Rh(CH_2CH_2)]^{\bullet}$ in toluene glass (90 K). (A) $^{12}CH_2{=}^{12}CH_2$: $\nu$ = 9.520 GHz, sweep width = 1000 G, $g_{xx}$ = 2.323, $g_{yy}$ = 2.222, $g_{zz}$ = 1.982, $A_{^{103}Rh(g_{xx})} \cong 72.5$ MHz, $A_{^{103}Rh(g_{yy})} \sim 65.0$ MHz, $A_{^{103}Rh(g_{zz})}$ = 102.4 MHz. (B) $^{13}CH_2{=}^{13}CH_2$: $A_{^{13}C(g_{zz})}$ = 37.9 MHz, $A_{^{13}C(g_{xx})} \sim A_{^{13}C(g_{yy})} < 5$ MHz. (C) Simulated anisotropic spectrum using the experimental parameters for $[(TTiPP)Rh(^{13}CH_2{=}^{13}CH_2)]^{\bullet}$ given in A and B.

the $^1$H NMR spectrum ($T$ = 295 K) and is identified by the $^1$H and $^{13}$C NMR spectra of the $^{12}$C and $^{13}$C ethene derivatives.[6]

Exposing a toluene solution of [tetrakis(1,3,5-triisopropylphenyl)porphyrinato]rhodium(II),[1] (TTiPP)Rh$^{\bullet}$ (**2**), to $^{12}C_2H_4$ and $^{13}C_2H_4$ (0.3 atm) and freezing (90 K) results in the EPR spectra shown in Figure 1. The $g_{zz}$ transition of the $^{13}C_2H_4$ derivative occurs as a doublet of triplets arising from nuclear hyperfine coupling with $^{103}$Rh ($A_{^{103}Rh(g_{zz})}$ = 102.4 ± 1.0 MHz) and two equivalent $^{13}$C ($A_{^{13}C(g_{zz})}$ = 37.9 MHz) nuclei in ethene, which identifies the species as a 1:1 ethene $\pi$ complex, $[(TTiPP)Rh(CH_2{=}CH_2)]^{\bullet}$ (**3**) (eq 2). Compound **3** has a formal

$$(TTiPP)Rh^{\bullet} + CH_2{=}CH_2 \rightleftharpoons [(TTiPP)Rh(CH_2{=}CH_2)]^{\bullet} \quad (2)$$

resemblance to paramagnetic ($s = {}^1/_2$) complexes of alkenes with metal atoms[7] and $[Fe(CO)_3]^{\bullet-}$.[8] Solutions that contain an equilibrium distribution of **2**, **3**, and ethene (296 K) react slowly over a period of days to form an ethene coupling product of (TTiPP)Rh analogous to **1**.

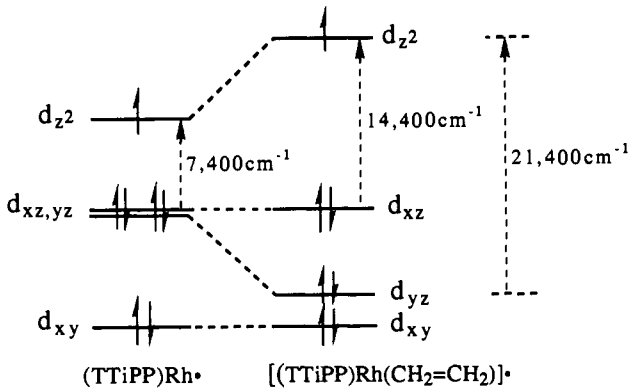


**Figure 2.** Schematic d MO diagram for (TTiPP)Rh$^{\bullet}$ and $[(TTiPP)Rh(CH_2CH_2)]^{\bullet}$ (**3**) derived from analysis of EPR parameters. The coordinate system for **3** is based on $C_{2v}$ symmetry where the $z$ axis is the $C_2$ axis normal to the porphyrin plane and the $yz$ plane is defined to contain the Rh, two ethene carbons, and two pyrrole nitrogens such that the $d_{yz}$ is the primary metal d$\pi$ donor orbital.

Estimates of the rhodium $d_{z^2}$ spin density ($\rho_{Rh(d_{z^2})} \sim 0.67$) and d orbital energy separations ($\Delta E_{z^2\leftarrow xz} \sim 14400$ cm$^{-1}$; $\Delta E_{z^2\leftarrow yz} \sim 21400$ cm$^{-1}$) for **3** are obtained by fitting the observed $g$ values and $^{103}$Rh coupling constants to expressions derived for a $d_{xy}{}^2 d_{xz,yz}{}^4 d_{z^2}{}^1$ ground configuration.[9,10] Analysis of the $^{13}$C coupling constants[11] provides estimates for the $C_{2p}$ (0.139), $C_{2s}$ (0.004), and total ethene carbon (0.286) spin densities. The d MO energy separations for **2** and **3** that are estimated from EPR $g$ and $\lambda$ values are illustrated in Figure 2.[10] Lowering of the $d_{yz}$ relative to the $d_{xz}$ by ~7000 cm$^{-1}$ is a direct consequence of the ethene $\pi$ acceptor interaction, and elevation of the $d_{z^2}$ in **3** from its position in **2** by ~7000 cm$^{-1}$ results from the $\sigma$ donor properties of ethene. The EPR parameters for **3** provide an experimental description of the metal–alkene binding that is consistent with theoretical models.[12-14]

Interaction of a radical (X$^{\bullet}$) with ethene to form substantial concentrations of an alkyl radical ($X{-}CH_2CH_2^{\bullet}$) requires an $X{-}CH_2$ bond dissociation enthalpy of approximately 72 kcal mol$^{-1}$.[15] Metalloradical reactions of (por)Rh$^{\bullet}$ species with alkenes differ from alkyl radical reactions in that the (por)Rh–$CH_2$ bond dissociation enthalpy (~50 kcal mol$^{-1}$)[3] is insufficient to justify formation of an authentic carbon-based alkyl radical intermediate ((por)Rh–$CH_2CH_2^{\bullet}$). Concerted formation of two Rh–$CH_2$ bonds is required for alkene reduction, and this feature provides the

(6) (TTEPP)Rh$^{\bullet}$ is generated by photolysis of (TTEPP)Rh–$CH_3$ in benzene as previously reported for the (tetramesitylporphyrinato)rhodium(II) radical.[1] Reaction of (TTEPP)Rh$^{\bullet}$ with $^{12}C_2H_4$ and $^{13}C_2H_4$ (~300 Torr) in benzene solution produces **1**, (TTEPP)Rh–$CH_{2(1)}CH_{2(2)}CH_{2(3)}CH_{2(4)}$–Rh-(TTEPP), which is identified in solution by $^1$H and $^{13}$C NMR. The $^1$H NMR spectrum of **1** at room temperature displays two broad overlapping resonances centered at –5.84 and –5.89 ppm assigned to the organometallic fragment ($CH_{2(1,4)}$ and $CH_{2(2,3)}$). The two proton resonances in the $^{13}$C derivative of **1** are further split by $^{13}$C ($^1J_{^{13}C-H_{(1,4)}} \approx 143$ Hz and $^1J_{^{13}C-H_{(2,3)}} \approx 126$ Hz). The proton-decoupled $^{13}$C NMR spectrum of **1** displays two well-separated resonances ($\delta_1$ = 27.48 ppm; $\delta_2$ = 13.85 ppm). The $^{13}$C resonance at $\delta$ = 13.85 ppm appears essentially as a triplet resulting from near-equivalent $^1J$ coupling to both $^{103}$Rh and $^{13}$C ($^1J_{^{13}C_1-^{13}C_2} = {}^1J_{^{13}C_3-^{13}C_4} \approx 30$ Hz; $^1J_{^{103}Rh-^{13}C_1} = {}^1J_{^{103}Rh-^{13}C_4} \approx 30$ Hz) and is assigned to $C_1$ and $C_4$. The $^{13}$C resonance at $\delta$ = 27.48 ppm appears as an AA'XX' pattern ($^1J_{^{13}C_1-^{13}C_2} + {}^2J_{^{13}C_2-^{13}C_4}$ = 31.5 Hz) and is assigned to $C_2$ and $C_3$.

(7) (a) Kasai, P. H.; McLeod, D., Jr.; Watanabe, T. *J. Am. Chem. Soc.* **1980**, *102*, 179. (b) Kasai, P. H. *J. Phys. Chem.* **1982**, *86*, 3684. (c) Kasai, P. H. *J. Am. Chem. Soc.* **1982**, *104*, 1165. (d) Kasai, P. H. *J. Am. Chem. Soc.* **1984**, *106*, 3069.

(8) (a) Krusic, P. J.; San Filippo, J., Jr. *J. Am. Chem. Soc.* **1982**, *104*, 2645. (b) Krusic, P. J.; Brière, R.; Rey, P. *Organometallics* **1985**, *4*, 801.

(9) McGarvey, B. R. *Can. J. Chem.* **1975**, *53*, 2498.

(10) Solving the expressions that relate the observed $g$ and $^{103}$Rh coupling constants with the d orbital energy separations $\Delta E_{z^2\leftarrow xz}$ ($\Delta E_1$) and $\Delta E_{z^2\leftarrow yz}$ ($\Delta E_2$), the effective spin–orbit coupling constant ($\lambda$), isotropic coupling constant ($K$), and dipolar coupling term ($P$) for $^{103}$Rh in the complex[9] results in the following parameters for **3**: $\lambda/\Delta E_1 = 0.0567$; $\lambda/\Delta E_2 = 0.0381$; $P$ = 63.9 ± 6 MHz; $K$ = 68.1 ± 6 MHz. The $P$ and $\lambda$ values in the complex are assumed to scale linearly with the rhodium $d_{z^2}$ spin density ($P/P_0 = \lambda/\lambda_0 = \rho_{Rh(d_{z^2})}$ where $P_0$ (95.9 MHz) and $\lambda_0$ (1220 cm$^{-1}$) are the free ion values for Rh(II)). The ratio of $P$ to $P_0$ yields the rhodium $d_{z^2}$ spin density ($\rho_{Rh(d_{z^2})}$ = 0.67) and the effective spin–orbit coupling constant ($\lambda = (P/P_0)(\lambda_0)$ = 817 cm$^{-1}$) for **3**. Evaluating the d orbital energy separations by using $\lambda$ = 817 cm$^{-1}$ results in $\Delta E_{z^2\leftarrow xz} \sim 14.4 \times 10^3$ cm$^{-1}$ and $\Delta E_{z^2\leftarrow yz} \sim 21.4 \times 10^3$ cm$^{-1}$ ($g_{xx} = g_{yy}$ = 2.823 for (TTiPP)Rh$^{\bullet}$; $\lambda/\Delta E_1 = 0.164$; for $\lambda_0$ = 1220 cm$^{-1}$, $\Delta E_1$ ~7400 cm$^{-1}$).

(11) Observation of equivalent ethene carbon atoms requires that **3** contain a 2-fold symmetry axis, which further requires that this axis ($z$ axis) be a principal direction for both the $g$ and $A_{^{13}C}$ tensors; $g_{xx}$ is assigned the largest $g$ value (2.323), which corresponds to the $d_{xz}$ being above the $d_{yz}$, in keeping with the dominance of the out-of-plane $\pi$ bonding and the assigned coordinate system (Figure 2). The $C_{2s}$ and $C_{2p}$ spin densities for **3** can be estimated from the relationships $A_{^{13}C_{zz}} = \langle A_{^{13}C}\rangle + 2B_{^{13}C}$, $\langle A_{^{13}C}\rangle/(3110$ MHz) = $\rho_{C_{2s}}$ and $B_{^{13}C}/(90.8$ MHz) = $\rho_{C_{2p}}$ using $A_{^{13}C_{zz}}$ = 37.9 MHz, $\langle A_{^{13}C}\rangle \sim A_{^{13}C_{zz}}/3 \sim 12.6$ MHz.

(12) Chatt, J.; Duncanson, L. A. *J. Chem. Soc.* 1953, 2939.

(13) Dewar, M. J. S. *Bull. Soc. Chim. Fr.* **1951**, *18*, C71.

(14) Mingos, D. M. P. Bonding of Unsaturated Organic Molecules to Transition metals. In *Comprehensive Organometallic Chemistry*; Wilkinson, G., Stone, F. G. A., Abel, E. W., Eds.; Pergamon: New York, 1982; Vol. 3, pp 1–88.

(15) Wayland, B. B. *Polyhedron* **1988**, *7*, 1545.

opportunity to achieve selectivity for metalloradical reactions. The large steric demands of (TTEPP)Rh prohibit formation of the two-carbon bridged complex, and the reaction proceeds to give a four-carbon alkene coupling product, **1**, which relieves the steric congestion. Alkene oligomerization stops at the dimer because further radical reaction requires homolysis of a relatively strong Rh–$CH_2$ bond. We are currently evaluating reactions for a wide variety of metalloradicals and alkenes in an effort to determine the generality and efficacy of this type of controlled radical process.

**Acknowledgment.** We are indebted to Dr. Alan E. Sherry for the synthesis of the (TTiPP)Rh–$CH_3$ and (TTEPP)Rh–$CH_3$ compounds used in this study to generate the metalloradicals. This work was supported by the National Science Foundation through Grant CHE-87-16691. Additionally, we thank the Science and Engineering Research Council, United Kingdom, for a studentship (to A.G.B.).

## Sub-Picosecond $\Delta S = 2$ Intersystem Crossing in Low-Spin Ferrous Complexes

James K. McCusker, Kevin N. Walda, Robert C. Dunn, John D. Simon,* Douglas Magde,* and David N. Hendrickson*

*Department of Chemistry, 0506*
*University of California at San Diego*
*La Jolla, California 92093-0506*

*Received March 30, 1992*

In this communication, we present observations on two $\Delta S = 2$ intersystem crossing processes for $Fe^{II}$ complexes, namely, the $^1MLCT \rightarrow {}^5T_2$ and $^5T_2 \rightarrow {}^1A_1$ conversions. Intersystem crossing where $\Delta S = 2$ has previously been examined for several $Fe^{II}$ complexes.[1,2] For spin-crossover $Fe^{II}$ complexes where the $^1A_1$ and $^5T_2$ "ligand-field" states are in close energy proximity ($\Delta E < 1000\ cm^{-1}$), excited-state relaxation times have been found to be in the range of 40–120 ns and assigned as $^5T_2 \rightarrow {}^1A_1$. The excited-state characteristics of low-spin $Fe^{II}$ polypyridyl complexes have also been examined in detail.[3] The $[Fe(bpy)_3]^{2+}$ complex is first photoexcited from the $^1A_1$ ground state to a singlet metal-to-ligand charge-transfer excited state, $^1MLCT$, where picosecond time-resolved studies[3c,d] suggest that the $^1MLCT$ state is depopulated in $\leq 10$ ps. By ground-state bleaching recovery experiments, a 0.81 ± 0.07 ns state of $[Fe(bpy)_3]^{2+}$ has been identified[3a,c] and tentatively assigned[3e] as a $^5T_2$ ligand-field state. In this work, results are presented which definitively establish the $^5T_2$ nature of the long-lived excited state in $Fe^{II}$ spin-crossover complexes and that depopulation of the $^1MLCT$ state occurs in <1 ps.

Previously we reported[4] that $[Fe(tpen)](ClO_4)_2$, where tpen is the hexadentate ligand tetrakis(2-pyridylmethyl)-1,2-ethylenediamine, is a spin-crossover complex both in the solid state and in solution. Following $^1MLCT \leftarrow {}^1A_1$ excitation of a $3.36 \times 10^{-4}$ M $H_2O$ solution of $[Fe(tpen)](ClO_4)_2$ at 440 nm at 290 K, transient bleaching was monitored at $\lambda = 430$ nm to determine a relaxation time of 18 ± 2 ns ($k = (5.6 \pm 0.6) \times 10^7\ s^{-1}$) (Figure 1).[5] The corresponding $^5T_2$ lifetime of 20 ± 2 ns is nearly a factor of 2 shorter than that reported for any other $Fe^{II}$ spin-crossover complex. Probe wavelengths in the 266–440 nm range were employed to establish as definitively as possible the identity of the excited state as the $^5T_2$ ligand-field state.[6] A change from transient absorption to transient bleaching was found at ~300 nm (i.e., $\Delta OD_{\lambda=300nm} \approx 0$). This wavelength coincides with an isosbestic point determined from variable-temperature static electronic absorption spectra.[7] Furthermore, a single kinetic species was observed in the picosecond experiment for all delay times spanning the instrument-limited response time (~50 ps)

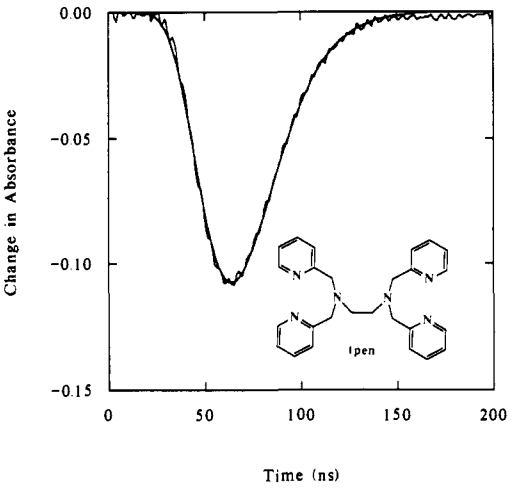


**Figure 1.** Transient bleaching observed at 430 nm for a $3.36 \times 10^{-4}$ M aqueous solution of $[Fe(tpen)](ClO_4)_2$ following excitation at 440 nm. The fit represents a convolution of the instrument response function with a single exponential decay ($\tau = 18 \pm 2$ ns).

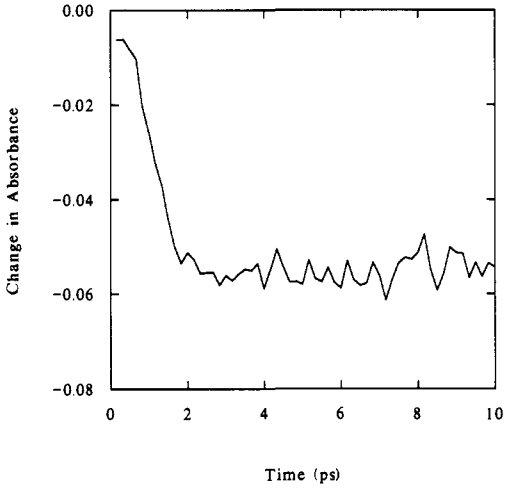


**Figure 2.** Plot of the change in absorbance [ΔOD] as a function of time in steps of 167 fs following $^1MLCT \leftarrow {}^1A_1$ excitation of a $1.52 \times 10^{-3}$ M aqueous solution of $[Fe(tpen)](ClO_4)_2$ at 314 nm. The width of the excitation pulse was ~500 fs.

(1) For recent reviews of dynamical studies on spin-crossover complexes, see: (a) Beattie, J. K. *Adv. Inorg. Chem.* **1988**, *32*, 1. (b) Konig, E. *Struct. Bonding* **1991**, *76*, 51.

(2) (a) Hauser, A.; Vef, A.; Adler, P. *J. Chem. Phys.* **1991**, *95*, 8710. (b) Hauser, A. *Coord. Chem. Rev.* **1991**, *111*, 275. (c) Hauser, A. *J. Chem. Phys.* **1991**, *94*, 2741. (d) Gutlich, P.; Poganiuch, P. *Angew. Chem., Int. Ed. Engl.* **1991**, *30*, 975. (e) Poganiuch, P.; Descurtins, S.; Gutlich, P. *J. Am. Chem. Soc.* **1990**, *112*, 3270. (f) Gutlich, P.; Hauser, A. *Coord. Chem. Rev.* **1990**, *97*, 1. (g) Figg, D. C.; Herber, R. H. *Inorg. Chem.* **1990**, *29*, 2170. (h) Conti, A. J.; Xie, C.-L.; Hendrickson, D. N. *J. Am. Chem. Soc.* **1989**, *111*, 1171. (i) Xie, C.-L.; Hendrickson, D. N. *J. Am. Chem. Soc.* **1987**, *109*, 6981.

(3) (a) Kirk, A. D.; Hoggard, P. E.; Porter, G. B.; Rockley, M. G.; Windsor, M. W. *Chem. Phys. Lett.* **1976**, *37*, 199. (b) Street, A. J.; Goodall, D. M.; Greenhow, R. C. *Chem. Phys. Lett.* **1978**, *56*, 326. (c) Creutz, C.; Chou, M.; Netzel, T. L.; Okumura, M.; Sutin, N. *J. Am. Chem. Soc.* **1980**, *102*, 1309. (d) Bergkamp, M. A.; Brunschwig, B. S.; Gutlich, P.; Netzel, T. L.; Sutin, N. *Chem. Phys. Lett.* **1981**, *81*, 147. (e) Hauser, A. *Chem. Phys. Lett.* **1990**, *173*, 507.

(4) Chang, H.-R.; McCusker, J. K.; Toftlund, H.; Wilson, S. R.; Trautwein, A. X.; Winkler, H.; Hendrickson, D. N. *J. Am. Chem. Soc.* **1990**, *112*, 6814.

(5) Nanosecond experiments were carried out using a XeCl excimer-pumped dye laser and a Xe flashlamp. Details of this variable-temperature facility will be reported in a forthcoming paper (McCusker, J. K.; Hendrickson, D. N. Manuscript in preparation).

(6) Short-wavelength probe experiments as well as all sub-nanosecond lifetime determinations were carried out using a mode-locked Q-switched and cavity-dumped Nd:YAG laser and a synchronously pumped dye laser; see: Xie, X.; Simon, J. D. *Opt. Commun.* **1989**, *69*, 303.

(7) The *apparent* isosbestic point of $\lambda = 326$ nm reported in ref 4 is incorrect due to a small amount of an impurity that was present in the solution.

0002-7863/92/1514-6919$03.00/0 